A comparative co-simulation analysis to improve the sustainability of cogeneration-based district multi-energy systems using photovoltaics, power-to-heat, and heat storage

Anselm Erdmann [a], Anna Marcellan [b], Jan Stock [c], David Neuroth [d,e], Christian Utama [f], Michael Suriyah [g], Sina Steinle [g], Felicitas Müller [g], Dominik Hering [c,h], Henning Francke [i,1], Sascha Gritzbach [j], Martin Henke [b], Noah Pflugradt [d], Hüseyin Çakmak [a], Leander Kotzur [d], Detlef Stolten [d,k], Thomas Leibfried [g], Dirk Müller [c,h], Rutger Schlatmann [f,l], André Xhonneux [c], Veit Hagenmeyer [a], Carolin Ulbrich [f,*]

[a] Institute for Automation and Applied Informatics, Karlsruhe Institute of Technology, Kaiserstraße 12, 76131 Karlsruhe, Germany
[b] Institute of Combustion Technology, German Aerospace Center, Pfaffenwaldring 38-40, 70569 Stuttgart, Germany
[c] Institute of Energy and Climate Research, Energy Systems Engineering (IEK-10), Forschungszentrum Jülich GmbH, Wilhelm-Johnen-Straße, 52428 Jülich, Germany
[d] Institute of Energy and Climate Research, Techno-economic Systems Analysis (IEK-3), Forschungszentrum Jülich GmbH, Wilhelm-Johnen-Straße, 52428 Jülich, Germany
[e] Chair VII for Computer Science, Faculty of Mathematics, Computer Science and Natural Sciences, RWTH Aachen University, Templergraben 55, 52056 Aachen, Germany
[f] PVcomB, Helmholtz-Zentrum Berlin für Materialien und Energie GmbH, Hahn-Meitner-Platz 1, 14109 Berlin, Germany
[g] Institute of Electric Energy Systems and High-Voltage Technology, Karlsruhe Institute of Technology, Kaiserstraße 12, 76131 Karlsruhe, Germany
[h] Institute for Energy Efficient Buildings and Indoor Climate, E.ON Energy Research Center, RWTH Aachen University, Templergraben 55, 52056 Aachen, Germany
[i] Helmholtz Centre Potsdam, GFZ German Research Centre for Geosciences, Telegrafenberg, 14473 Potsdam, Germany
[j] Institute of Theoretical Informatics, Karlsruhe Institute of Technology, Kaiserstraße 12, 76131 Karlsruhe, Germany
[k] Chair for Fuel Cells, RWTH Aachen University, c/o Institute of Techno-economic Systems Analysis (IEK-3), Forschungszentrum Jülich GmbH, Wilhelm-Johnen-Straße, 52428 Jülich, Germany
[l] Faculty 1: School of Engineering – Energy and Information, HTW Berlin–University of Applied Sciences, 10313 Berlin, Germany

ARTICLE INFO

This paper is dedicated to the memory of our dear co-worker Henning Francke.

ABSTRACT

For an extensive decarbonization of district multi-energy systems, efforts are needed that go beyond today's cogeneration of heat and power in district multi-energy systems. The multitude of existing technical possibilities are confronted with a large variety of existing multi-energy system configurations. The variety impedes the development of universal decarbonization pathways. In order to tackle the decarbonization challenge in existing and distinct districts, this paper calculates a wide range of urban district configurations in an extensive co-simulation based on domain specific submodels. A district multi-energy system comprising a district heating network, a power grid, and cogeneration is simulated for two locations in Germany with locally captured weather data, and for a whole year with variable parameters to configure a power-to-heat operation, building insolation/refurbishment, rooftop photovoltaic orientation, future energy demand scenarios, and district sizes with a temporal resolution of 60 s, in total 3840 variants. The interdependencies and synergies between the electrical low-voltage distribution grid and the district heating network are analysed in terms of efficiency and compliance with network restrictions. Thus, important sector-specific simulations of the heat and the electricity sector are combined in a holistic district multi-energy system co-simulation. The clearly most important impact on emission reduction and fuel consumption is a low heat demand, which can be achieved through thermal refurbishment of buildings. Up to 46 % reduction in CO_2 emissions are possible using the surplus electricity from photovoltaics for power-to-heat in combination with central heat storage in the district's combined heat and power plant. Domestic hot water heated by district heating network in combination with power-to-heat conversion distributed in the district reduces the load on the distribution power grid. Even though the

---

* Corresponding author.
  E-mail address: carolin.ulbrich@helmholtz-berlin.de (C. Ulbrich).
  [1] Deceased author.

investigated measures already improve the sustainability significantly, providing the energy needed for the production of synthetic fuels remains the crucial challenge on the further path towards net-zero.

Nomenclature	
MGT	Micro gas turbine
CHP	Combined heat and power plant
PtH	Power-to-heat
PV	Photovoltaics

1. Introduction

Combined heat and power in conjunction with a district heating network is a well-known way of efficiently supplying heat and electrical power. However, heat as a large part of private energy consumption is still often generated by burning fossil fuels. Due to the dependence on fossil fuels and the emissions inherent in the system, further improvements of district heating networks are clearly needed and are therefore increasingly being investigated [1–3].

For the decarbonization of the energy system, electricity is seen as the major driver [4] and will be generated in even greater quantities in the future at low cost from sunlight, among other sources [5]. PV is an important source of energy available within residential areas. Its fluctuating nature can, however, become challenging for the electrical grids [6]. Thus, measures that avoid transmission and use local storage options enable an increased local PV deployment [7]. For the integration of PV, district multi-energy systems are of particular interest, as the high thermal inertia of water and the resulting flexibility of heat storage provide low-effort on-site integration support when surplus PV power is converted into heat. For existing districts and infrastructure, the attributed endeavour of infrastructural reconstruction requires customized solutions. Technical solutions to reach carbon neutrality in districts are vast. Every single measure, yet, has an influence on the complex system. Besides the intended reduction of emissions, the resource demand changes. Efficiency, autarky, and operational stability are also directly affected. The present contribution quantifies the impacts of single measures in respect to sustainability aspects. A quantification is an essential requirement for a holistic impact assessment. Therefore, in this contribution a district multi-energy system is analysed in various configurations varying structural system conditions, construction measures, and future trends. The presented work is a simulation-based study to analyse the cross-sectoral impact of different options and configurations on the sustainability, resources, and efficiency of future district multi-energy systems. The focus is on multi-energy systems at district level according to [8]. It is assumed that the district itself already exists with inhabited buildings and surrounding infrastructure comprising a stand-alone district heating network with mini CHP and an electrical distribution grid. As a low-threshold measure, it is assumed that rooftop PV is already installed on all buildings. In the selected geographical location of Central Europe, the days with high PV generation are mainly between spring to autumn. Heating of buildings is mainly needed during the cold and less sunny winter months.

Table 1 gives an overview of scenario parameters under consideration. These can be divided into the three categories: construction measures, structural conditions, and future trends. First, construction measures are investigated. On the building side, various insulation states, and methods for domestic hot water supply (by district heating network or electrical) are considered. As an important cross-sectoral technology for district multi-energy systems, the integration of power-to-heat is extensively investigated. The influence of power-to-heat on selected key performance indicators is considered in a decentralized

variant with power-to-heat units within the buildings, and in a centralized variant with energy conversion in the CHP by means of direct electric heating. All these construction measures avoid long-term disruptions in every-day life caused by huge reconstructions.

Second, different structural conditions are taken into account. The district multi-energy system is modelled in two district sizes, each at two exemplary locations in Germany, and each with two different building roof orientations, which influences the shape of the generation profiles and the amount of PV generation.

Third, as possible future trends, implementing air conditioning and inner-city mobility with individual BEVs are considered.

The novelty of this work is the creation of comparability between a high number of parameter variations using extensive, high-detailed simulations developed by domain experts and considering a full year. In order to cover interdependencies, impacts, and cross-sectoral synergies between the different sectors, the representation of simultaneity is ensured by using a high temporal resolution. The energy consumption is modelled in spatial resolution of the individual buildings. Additional efforts in order to achieve net-zero are calculated.

The remainder of the article is organized as follows: Section 2 gives a literature overview on decarbonization studies with integration of renewable energy sources at district level using power-to-heat. Section 3 comprises the simulation-based method and details about the developed simulation models and the used software. It starts with an introduction of the parameter set for all variations under consideration in Section 3.1, which is referenced in the remaining sections. The results are presented in Section 4 and discussed in Section 5. Finally, this work is concluded in Section 6.

2. District multi-energy systems using the flexibility of heat for the integration of renewables

The integration of renewable energy sources in district energy systems is both a challenge and an opportunity. Dense cities need to import a lot of energy. However, heating in urban areas can also provide additional flexibility to the environment, thereby damping fluctuations in renewable energy generation. The expansion of multi-energy systems for the integration of renewable energy resources needs to study operational details already during the planning phase [9]. To this end, simulation is the method required (Section 2.1) which is applied in various application cases (Section 2.2).

2.1. Simulation as a predestinated method

The different behaviour of connected energy forms in multi-energy systems provides flexibility and allows to mitigate fluctuations between energy generation from volatile energy resources and energy demand [9]. Photovoltaics as a renewable energy source that is locally available even in dense urban areas is highly volatile. At the same time, space heating and domestic hot water are locally available flexibility options [7]. Heat and power cogeneration in combination with district heating systems is a well established concept [2,10] with established methods and models, but is facing new challenges [11]. The integration of highly volatile renewable energy resources requires a high temporal resolution in order to represent matching between energy demand and supply sufficiently [12].

In contrast to optimization approaches where the system is controlled for an optimized operation according to one specific objective function (e.g. cost minimization), the present contribution aims to examine a range of impacts represented by different sustainability indicators. Many scenario configuration variables have to be varied and therefore require a simulation approach that is not optimized for one specific configuration.

Table 1
Considered scenario parameters for district multi-energy systems in this work.

Category	Scenario parameters under consideration
Construction measures	Building insulation Domestic hot water supply Power-to-heat integration
Structural conditions	Location Roof-PV orientation District size
Future trends	Dissemination of mobility with battery electric vehicles Dissemination of air conditioning Fuel decarbonization

2.2. Case studies

The arrangement of district multi-energy systems and thus also accompanying challenges and research questions can be very different. In traditional district multi-energy systems, the energy flow starts from a gas network and an electricity grid at the system boundaries and reaches the end use of heat and electricity through one or more of the many different possible conversions [13]. Evolving residential PV generation poses new challenges to distribution grid capacity (see [6,7]), but district heating systems can provide the required flexibility by using power-to-heat on site. The remaining fuel demand in the district heating systems is in turn reduced by power-to-heat.

Power-to-heat and the associated interdependencies in district multi-energy systems have been investigated by several case-studies. Table 2 shows case studies of district or regional energy systems considering the integration of renewable energy resources and power-to-heat. Some studies [7,14,19] use cost minimizing optimization methods, the others use simulation-based approaches. The presented works consider district multi-energy systems including power and heat. Most of them [6,7,14–17,19–21] consider the integration of renewable energy resources as wind power and PV for heating. Cross-sectoral effects need the consideration of both the electrical and the heat side. Restrictions in the low-voltage distribution grid are particularly considered by [6,7,15].

The very different locations complicate direct comparisons. Different climatic conditions influence both the demands and the generation of renewable energy. The studies [19,21] also consider cooling in their multi-energy system.

Salpakari et al. [14] present a case-study for the integration of renewable energy sources into the district heating system of Helsinki. As renewable energy resources, city-near wind power and PV are considered. Note that PV generation is low at the high latitude of 60° North compared to other regions and the number of daylight hours is extremely different between summer and winter. The high availability of wind power makes this study very site specific. The energy system uses power-to-heat (heat pumps and electric boilers) in combination with thermal storage and demand side management as flexibility options. Power-to-heat achieves a share between 82% and 93% of the total heat production. The focus of [14] lies on a detailed economical investigation of possible configurations for energy conversion measures.

Widl et al. [15] consider a district with 135 buildings located in southern Germany, 80% with rooftop PV. They compare ecological and economical operational strategies for power-to-heat using simulation. The multi-energy system consists of a district heating network with a $135\,m^3$ heat storage tank and a power grid. An electric boiler enables the conversion of surplus power into heat. The district heating network is a sub-network of a large city district heating in which heat can be exchanged to an unlimited extent. This assumption allows to consider the full power-to-heat capacity in the dedicated district. However, scaling the results to the whole city district heating system requires further research, since the low heat demand in summer limits the consumption and, thus, the power-to-heat capacity.

The studies [16,17] determine the potential of power-to-heat in district heating networks as a flexibility measure for negative residual loads. The renewable energy generation is not located within the districts and needs transport capacities to the districts, which itself are not modelled. Schweiger et al. [16] consider scenarios for the electricity production development in Sweden. The national negative residual loads for these scenarios and the flexibility options by power-to-heat using electric boilers in the district heating systems are examined. The impact of thermal heat storage, industrial waste heat, and years with different weather conditions on the power-to-heat potential are determined. Remarkable is the consideration of combinations of measures and their interdependencies. Depending on the scenario, between 59% and 89% of the negative residual load could be used for power-to-heat. However, the focus lies on the avoidance of negative residual loads and covers only about 11% of the total annual heat demand in Swedish district heating systems. Böttger et al. [17] determine the corresponding power-to-heat potential for Germany. The potential is simulated for the projected renewable energy generations in five-year steps up to 2030. Heat storage is not considered. The authors identify a power-to-heat potential between 37% and 42% of the negative residual load in the year 2030. This corresponds to 9% of the assumed annual district heating heat demand of $98.2\,TWh$.

Kontu et al. [18] examine the national potential for power-to-heat using heat pumps in Finland's district heating networks. Three different sizes of district systems are considered and supplemented with heat pumps in different capacities. They assume the heat supply by CHPs and heat only boilers where the heat is generated by biofuel (base load) and fossil fuels (peak load). The heat supply is supplemented by additionally installed heat pumps and the economical potential investigated at different electricity prices. Unfortunately, the results for the different district sizes are not directly comparable, since small district heating systems use heat only boilers for the heat supply, large systems, in contrast, use more efficient CHPs.

The integration of the thermal flexibility in district multi-energy systems from the economical control perspective is investigated by Capone et al. [19]. The considered multi-energy system is located in northern Italy and comprises thermal loads, cold loads and electricity loads. Heat is generated by CHP, heat boiler, and heat pump. Electricity is generated locally by PV and exchanged with the external grid. The economical impact is determined in configurations with thermal storage and demand side management up to $1\,h$ anticipation. Due to the high complexity of the optimization, the results for the complete year are extrapolated from four representative days in different seasons.

Similarly, Fambri et al. [20] analyse the district heating operation with additional power-to-heat in northern Italy. Power-to-heat plants equipped with heat pumps can preheat the water in the return flow or charge the thermal storage tank. The district multi-energy system is simulated for one year in $15\,min$ time steps. An optimized operation case provides flexibility to the electricity grid and achieves a reduction of the renewable energy overproduction by 40%.

For the construction of new district heating networks, the operation at low temperatures and additional heat pumps may be an option. The fluid serves as thermal source for heat pumps located close to the consumers [22]. The provided fluid temperature enables a high coefficient of performance. Such a multi-energy system using a low-temperature district heating and cooling network together with rooftop combined photovoltaic solar thermal panels is simulated and analysed for three European locations in [21]. The district heating and cooling network connects seven buildings each with six housing units. Heat supplied by the combined photovoltaic and thermal panels is used for domestic hot water. A heat exchanger feeds heat into the district heating network and cools the modules down at once. A heat pump connected to the district heating network at its source side heats the building.

Using the flexibility of heat is also possible, if no district heating is available. However, the heat cannot be stored centrally for the

Table 2

Overview of case-studies with the varied variable(s) under consideration. PtH: power-to-heat, TES: thermal energy storage, DSF: demand side flexibility, VRE: variable renewable energy, PVT: photovoltaic-thermal collectors, HP: heat pump (for space heating), BEV: battery electric vehicle. Heat pumps used for power-to-heat in district heating networks are listed under PtH.

Reference	Technologies	Wind	PV	Location	Variations
Salpakari et al. [14]	PtH, TES, CHP, DSF	Yes	Yes	Finland	VRE, TES, PtH, control
Widl et al. [15]	PtH, TES	No	Yes	Germany	Control
Schweiger et al. [16]	PtH, TES, CHP, waste heat	Yes	Yes	Sweden	VRE, PtH, TES, waste heat, weather
Böttger et al. [17]	PtH, CHP	Yes	Yes	Germany	VRE
Kontu et al. [18]	PtH, CHP	No	No	Finland	DHN size, electricity price
Capone et al. [19]	PtH, TES, CHP, DSF	No	Yes	Italy	TES, DSM
Fambri et al. [20]	PtH, TES, CHP	Yes	Yes	Italy	Control
Bordignon et al. [21]	PVT, TES	No	Yes	Finland, Germany, France	Location
Rinaldi et al. [7]	HP, DSF, PtH, el. storage	No	Yes	Switzerland	Building type, flexibility options, year
Gupta et al. [6]	HP, BEV	No	Yes	Switzerland	PV, HP, BEV

whole district but needs to be stored locally in each building and requires therefore smart grid communication infrastructure. Rinaldi et al. [7] compare various flexibility options like storage, power-to-heat (space heating and domestic hot water) or demand side response in terms of their capability to support the integration of PV in Swiss residential areas. The load shift of conversion into heat at times with high PV generation increases the self-consumption and enables thus the installation of more PV generation capacity.

Gupta et al. [6] consider the impact of heat pumps, battery electric vehicles (BEVs), and PV on the low-voltage distribution grids in Switzerland. The model comprises 170,000 households and considers the reinforcement of transformers and lines required for a stable operation of the energy system in scenarios with different penetration of PV, BEVs, and heat pumps. In the most aggressive penetration scenario, 14% of the transformer stations need to be rebuilt. However, exploiting the flexibility of heat by shifting heat loads is not considered as a flexibility option.

2.3. Research gap

All presented works investigate district multi-energy systems in multiple configurations by varying one or little more configuration parameters in order to attribute their impact. However, interdependencies between multiple implemented measures can distort the result in contrast to an isolated consideration (e.g. shown in [16] for storage and waste heat). Furthermore, most publications consider either the heat side or the power grid side in detail. However, for a deeper understanding of the interdependencies caused by power-to-heat, a detailed modelling of both sides and their restrictions is required. Hence, in order to cover the interdependencies of measures, of configurations, and those between the heat and the power system, we use detailed network models on both sides, vary multiple configuration parameters and simulate all configurations.

3. Methodology

In order to enable an extensive analysis of impacts of the considered measures towards more sustainability in district multi-energy systems, we opt for a simulation-based approach (see Section 2.1).

Highly detailed technical models are essential for the planning and operation of the future energy system [9,23]. Furthermore, as already noted by Rinaldi et al. [7], energy system models including flexibility need a sufficient granularity in order to represent synergies and enable trade-offs.

The present contribution is built on highly detailed technical models which are developed by domain experts that cooperated to advance district multi-energy systems. As the methods differ in the concerned domains, the district multi-energy system is composed of subsystem models in a co-simulation. The variety of configurations is added to the co-simulation as parameters.

Table 3

Overview of the varied parameters. Every meaningful combination of the eleven parameters is simulated.

Pos.	Parameter, associated values
(1)	District
(1.1)	District 16
(1.2)	District 48
(2)	Building type
(2.1)	Old (year of construction 1960, not refurbished)
(2.2)	Medium (year of construction 1990, not refurbished)
(2.3)	Modern (year of construction 2015, not refurbished)
(2.4)	Refurbished (year of construction 1960, fully refurbished)
(3)	Power-to-heat operation mode
(3.1)	No power-to-heat
(3.2)	Peak shaving power-to-heat
(3.3)	Surplus power-to-heat
(4)	Power-to-heat location
(4.1)	Distributed
(4.2)	Central
(5)	Domestic hot water supply
(5.1)	District heating network
(5.2)	Power grid
(6)	Micro gas turbine fuel
(6.1)	Natural gas
(6.2)	Syngas
(6.3)	Hydrogen
(7)	Mobility
(7.1)	No battery electric vehicles
(7.2)	Battery electric vehicles (used for inner-city routes)
(8)	Air conditioning
(8.1)	No air conditioning
(8.2)	Air conditioning
(9)	PV configuration
(9.1)	South, 40° inclination, 6.8 kW peak power
(9.2)	East and west, 40° inclination, 6.8 kW peak power per roof side
(10)	Location
(10.1)	Berlin-Adlershof, Helmholtz-Zentrum Berlin
(10.2)	Eggenstein-Leopoldshafen, Karlsruhe Institute of Technology
(11)	CHP connection
(11.1)	Transformer
(11.2)	Inside

3.1. Considered configuration parameters

Due to many changeable parameters in the development of the respective district energy system and the different accompanying impacts, this contribution investigates a broad variety of parameter sets by simulation. The basis of all considerations is a district multi-energy system comprising a district heating network, a power grid, and a mini CHP. An overview of all parameters and the associated values is given in Table 3.

A total of 9216 variations would theoretically be possible by combining all possible combinations of the measures, structural conditions, and possible future trends. Redundant variations and such in which the
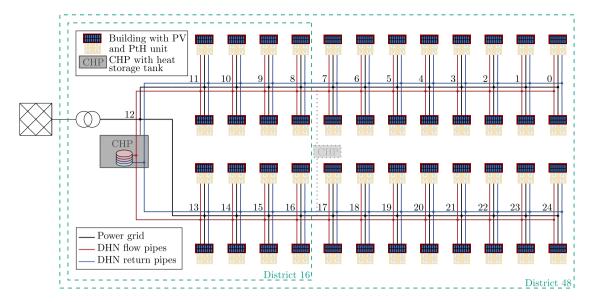
Fig. 1. District overview. A district heating network (DHN) and a power grid connect all buildings. The heat is supplied by a CHP with heat storage tank and additionally by power-to-heat centrally in the CHP or distributed in the buildings respectively. Electrical power is supplied by rooftop PV, in the CHP, and by import from the external grid. An alternative electrical connection of the CHP is displayed light grey.
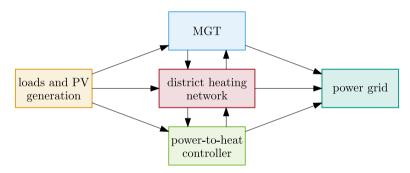

Fig. 2. Co-simulation setting. Previously simulated time series for heat demand, power demand, domestic hot water demand, and PV generation are used as input. These are fed to the simultaneously simulated models of the energy networks, control and facilities. The arrows represent the information flow. For a detailed presentation of the modelled energy flow between the simulators and subcomponents, see Supplementary Figure 1.

heat demand cannot possibly be covered due to the maximum power limit of the heat supply are skipped. All remaining 3840 meaningful variations are finally simulated.

The base scenario is varied in two district sizes (parameter (1)) at two locations (parameter (10)), with different roof orientations (parameter (9)), and different configurations of the electrical power grid (parameter (11)). The domestic hot water supply can be provided by the district heating network or by the electrical power grid (parameter (5)). Parameters concerning measures are building insulation (parameter (2)), additional power-to-heat facilities (parameter (4)), the corresponding operation strategy (parameter (3)), and different fuels for the heat supply (parameter (6)). To consider future changes in lifestyle with impact on the energy system, scenarios with BEVs (parameter (7)) and air conditioning (parameter (8)) are considered.

Obviously, there are many more possibilities with differently equipped buildings. Due to the countless possibilities, this work mainly simulates the extreme cases of fully or not equipped cases, which are expected to have the greatest impacts. The scenario is varied in multiple parameters for the base configuration, measures and future trends.

3.2. District energy system

In this contribution, a benchmark-district is considered in two sizes (parameter (1)). The district is based on the DESTEST (District Energy Simulation Test Procedure) district [24]. DESTEST forms a benchmark

to test and validate various simulation modules on urban-scale. In this contribution, the layout of the DESTEST district heating network is used since it provides a district reference case.

Fig. 1 gives an overview of the modelled district. District 16 (1.1) comprises the DESTEST network with 16 connected buildings and a mini CHP. District 48 (1.2) is an extension of the network layout of the District 16 case with overall 48 buildings. The scope is chosen to achieve a balance between heat supply capability and heat demand for various connected building heat demands (2). All buildings in the investigated district are connected to the district heating network. In addition, the electrical grid is also installed along the district heating network layout and thus has the same size as the district heating network.

The CHP is equipped with a MGT for power and heat cogeneration, which is connected to a $50\,m^3$ heat storage tank. Additionally, the conversion of electrical power into heat is possible using direct electric heaters (parameter (4)) distributed to all buildings (4.1), or next to the storage tank centrally in the CHP (4.2). In the central case, the required electrical power for the heating is transmitted from the buildings PV system via the electrical distribution grid to the CHP. In the alternative distributed configuration, the heated fluid is transmitted via the return pipes of the district heating network to the heat storage tank in the CHP. The incoming fluid is heated to a target temperature of 95 °C by power-to-heat in both configurations.

The electrical low-voltage distribution grid is modelled according to the structure of the district heating network consisting of two feeders with eight households connected to each feeder. The cable type NAYCWY $3 \times 150/150$ is used for the lines with a length of $108\,m$ ($300\,m$ for District 48 respectively) for each feeder. The households are connected along each feeder via a NAYCWY $3 \times 50/50$ cable with $12\,m$ at each household connection. The medium voltage busbar of a $0.4\,kV/20\,kV$ transformer represents the slack bus with fixed voltage magnitude of 1 p.u. and a voltage angle of $0°$. The CHP unit is directly connected (parameter (11)) to the busbar of the transformer (11.1). In an alternative setup, it is connected inside the grid (11.2) (see Fig. 1, light grey displayed CHP in the centre).

3.3. Simulation interfacing and setup

The district multi-energy system simulation comprises multiple simulations of subareas. Fig. 2 gives an overview of the setting.

At first, coherent time series for heat, electricity, domestic hot water, and PV generation are simulated using various tools (see Section 3.6). The calculated profiles are only influenced by the weather and the inhabitants' behaviour, but not by the energy system itself and can thus be simulated independently. The energy system is simulated in a co-simulation, that is split into simulation modules for the district heating network, the power grid, the MGT, and the power-to-heat control. The simulation modules synchronize their state after each time step. The division of the model content on the simulation modules is carried out with regard to the software used for model development.

The simulation modules are very heterogeneous as is the associated domain-specific software. Modelling the whole multi-energy system in a single tool would require a disproportionate re-developing effort for many models. In the literature, the use of one single tool for this purpose is quite unusual [23]. The crucial benefit of co-simulations is the possibility to combine different tools that are well-suited for the respective purpose [15]. Most software tools provide a programming interface, but the co-simulation standard *Functional Mockup Interface* [25] is not supported comprehensively. Hence, the interfaces between the simulations of the multi-energy system are specified comprehensively from the semantic side (top layer), which describes the multi-energy system's configuration, to the individual simulation software adaptation (bottom layer) as introduced in [26]. Each single variable is associated with a unit. The output variables are transferred after every simulation time step to the central co-simulation master. From there, the variables are distributed according to the configuration of the co-simulation and converted into the target unit of the associated input.

The high computational effort accompanying the required sub-hourly time series representation (see [9]) is met with high parallelization and reuse of already calculated redundant simulation parts from other variations.

3.4. General simulation time span and temporal resolution

The simulation setup is a trade-off between accuracy and computational effort. In order to cover the seasonality, a complete year is simulated. The temporal resolution is oriented to the electrical side. The scheduling of distributed renewable resources requires a sufficiently high temporal resolution to avoid disturbing influences of aggregation [9,27,28]. For PV systems at district level, a temporal resolution of $60\,s$ is recommended by Bucher et al. [28]. In district multi-energy systems, this resolution is very rarely applied; a temporal resolution of one hour is more common [9,29].

The common method of reducing the computational effort using representative time steps (see [9,19,30]) is not applicable, since the intra-day heat storage behaviour is of utmost importance in power-to-heat scenarios. Hence, the considered year is simulated completely in full time series representation.

Therefore, a period of one year (July 2019 to June 2020) is simulated in sub-hourly time series representation (according to [9]) with

a temporal resolution of $60\,s$ for two geographical locations (see Section 3.6).

3.5. Infrastructure simulation

The infrastructure simulations consist of the energy grid simulations, and simulations of the intermediate cross-network facilities MGT and direct electric heaters for power-to-heat conversion.

3.5.1. Grid simulations

The district heating network is modelled according to the network layout (see Section 3.2) as a dynamic district heating network simulation in Modelica®. The district heating network consists of different components like distribution pipes, which are modelled as subcomponents and later combined to form the district heating network simulation model. The required subcomponent models are obtained from the open source Modelica® library AixLib [31], which offers models for building and district heating simulations. The dynamic pipe model and the heat storage system are used from the AixLib model library. The heat storage tank is connected to the flow line and to the return line of the network and is supplied by the CHP and by distributed power-to-heat via the return line.

The power grid is modelled using the PYPOWER-based open source python tool Pandapower [32]. For performance reasons, the PYPOWER case file is extracted from Pandapower. Then, in every simulation time step, the current load and generation is updated in the PYPOWER case file. The low-voltage distribution power grid is simulated by a steady state AC power flow using PYPOWER, which is a Python implementation of MATPOWER [33].

3.5.2. Cross-network facilities

The CHP simultaneously supplies both electrical power to the power grid and heat to the heat storage tank which is connected to the district heating network. The CHP contains a MGT of type AE-T100/Dürr CPS with a maximum thermal power of $180\,kW$ and a maximum electrical power of $100\,kW$. While the conventional MGT operates with natural gas, the DLR institute of combustion technology developed a range of adapted burners that enable operation with various fuels [34–36]. The MGT is simulated with the MGTS[3] in-house simulation tool [37] with three different fuels (parameter (6)). Natural gas[2] (6.1) is the current standard. As carbon neutral alternatives syngas[3] (6.2) and pure hydrogen (6.3) are considered. To validate the developed model, the real MGT is evaluated in terms of efficiency, fuel consumption, and emissions in an experimental setup [38]. For this, the MGT is operated stably with gas mixtures from 100% syngas to 100% natural gas using one burner. Pressures, mass flows, and emissions are recorded at various locations. The case of 100% hydrogen combustion is then calculated numerically based on the previous model, which includes detailed models to consider effects of changes in fuel gas composition.

Additionally, there is the possibility to convert surplus electrical power to heat using ideal direct electric heaters. In comparison to heat pumps, direct electric heaters can be integrated in an existing infrastructure more easily and require little investment. The direct electric heaters within the single buildings in the distributed power-to-heat generation configuration (4.1) are implemented in the Modelica® model of the district heating network (see Fig. 2). In the power-to-heat configuration with one central direct electric heater located in the CHP (4.2), the power-to-heat controller calculates the mass flow required to heat up the fluid with the given power to a given setpoint temperature. The resulting mass flow rate is added to the mass flow rate coming from the MGT simulation and serves as an input for the district heating network simulation.

---

[2] Calorific value: $49.9\,MJ/kg$; gas mixture: 98.0 vol. % CH_4, 1.6 vol. % C_2H_6, 0.4 vol. % C_3H_8

[3] Calorific value: $7.4\,MJ/kg$; gas mixture: 32.0 vol. % H_2, 32.0 vol. % CO, 18.0 vol. % CO_2, 18.0 vol.% N_2
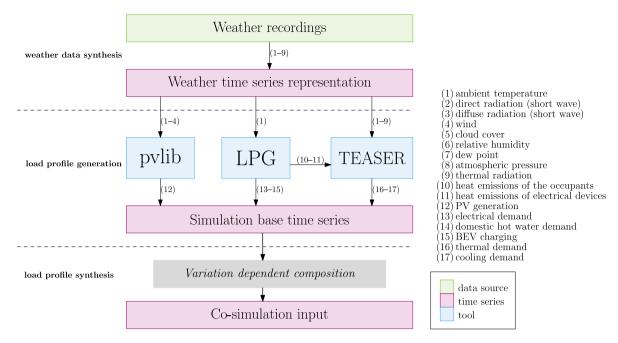
Fig. 3. The coherent co-simulation input time series consisting of PV, electrical, thermal, and domestic hot water profiles are calculated using weather data as input. For the calculation of the load profiles the open-source tools LoadProfileGenerator (LPG) and TEASER are used.

3.6. Coherent time series for PV, heating demand, and electrical demand

Unfortunately, the availability of real measured time series comprising PV, heating demand, and electrical demand for a whole district in a high temporal and spatial resolution is low. Therefore, the required load and generation profiles are generated synthetically.

Consumer load profiles and PV generation depend on the weather and the consumer's behaviour. However, they do not depend on the state of the multi-energy system's grids and are therefore calculated independently.

The availability of extensive weather data is the base for coherent multi-energy system time series. This comprises temperature, wind, pressure, humidity, long- and shortwave irradiation. The weather data were captured predominantly in weather stations (parameter (10)) of the Helmholtz-Zentrum Berlin in Berlin-Adlershof, Germany (10.1) and the Institute of Meteorology and Climate Research, Karlsruhe Institute of Technology in Eggenstein-Leopoldshafen, Germany (10.2). Since the captured data sets are not complete, a weather data synthesis using other data sources is performed. Missing data due to outages or not captured data are supplemented with measurements from the nearest weather station of the DWD Climate data centre [39] and ERA5 reanalysis data of the Copernicus Climate Data Store [40].

Fig. 3 shows the toolchain of the whole weather data and load profile synthesis. The weather station in Berlin-Adlershof is located on the rooftop of a building. It is surrounded by a mix of industrial, residential, and school buildings. The weather station of the Karlsruhe Institute of Technology is located at Campus North about 10 km north of Karlsruhe. The campus is surrounded by a forest.

On the base of the weather data, the time series for PV, electrical power demands, and thermal power demands are calculated. PV generation is calculated using the open source simulation tool pvlib [41]. All PV systems on the rooftops are assumed to have a peak power of 6.8 kW per roof side. Two configurations (parameter (9)) are considered in the simulation: in configuration (9.1), only the south-facing roof sides are equipped with PV and in configuration (9.2), the buildings are rotated by 90° and the east-facing roof sides as well as the west-facing roof sides are equipped with PV. In total 13.6 kW peak power are installed in configuration (9.2) compared to 6.8 kW in (9.1). In both cases, it is assumed that the roofs, respectively the modules, are tilted at a 40°

angle. All PV systems are assumed to be able to control their reactive power output in dependence on the active power output through the inverters in accordance with the German grid code [42].

In order to obtain all required household load profiles, the open source software LoadProfileGenerator (LPG) [43] is used. It uses an agent-based behaviour simulation model which allows to generate various types of coherent and plausible load profiles for individual households. The model is based on the residents' needs and does not depend on calibration data. This makes the simulation highly customizable, one can e.g. easily add BEVs to a household. A set of common German households has already been predefined and validated (for details see [44]). Out of those, 16 households are selected in accordance with statistical data from the German statistical federal authority [45] to form a representative set. As for the scenarios with BEV (parameter (7)), one BEV used for inner-city routes and one 3.7 kW charging station per household is assumed (7.2).

The LPG receives the same temperature profiles as used for the PV simulation and the heat demand simulation as input. As a result, the LPG delivers separate time series for each household. The time series comprise electrical power demand and domestic hot water demand as well as information on the heat emissions from residents and electrical devices. PV and load profiles serve directly as inputs for the district co-simulation. For the power calculation of the warmed up domestic hot water, a temperature increase of 30 K is assumed. These domestic hot water power profiles are added depending on parameter (5) to the thermal demand profiles (5.1) or to the electrical demand profiles (5.2).

The heat demand of buildings in districts can vary as the buildings differ in shape, year of construction, or type of usage, which leads to individual heat demands. Therefore, various building types with different years of construction and refurbishment states are taken into account (parameter (2)). These building types are adopted from typical buildings of the German building stock, which are characterized and parametrized in [46]. The following building types are parametrized: Old (built in 1960) (2.1), Medium (1990) (2.2), Modern (2015) (2.3), and Refurbished (1960, fully refurbished) (2.4). However, the heat demand of the parametrized building types not only depends on their geometry, physics, and usage type, but also on boundary conditions such as weather conditions or heat input from occupants or electrical devices. Therefore, weather data and heat emissions of inhabitants and

Table 4
Key performance indicators used for the comparison of the impact in different scenarios.

Category	Main indicator			Auxiliary indicator
	Description	Symbol	Unit	
Climate change impact	Direct carbon dioxide emissions	CO2	t	
Resource scarcity	Fuel consumption	FC	t	
Overall system efficiency	Heat generation	HG	MWh	
Degree of autarky	Energy import from the external power grid	EI	MWh	Energy export EE
Power quality	Voltage not exceeded 95% of time at line end	U95	p.u.	

electrical devices serve as input data for the simulation of the buildings' heat demands (see Fig. 3).

The buildings are simulated, assuming different building types to account for the different heat demands connected to the grid. The setpoint for the room temperature is assumed to be 20 °C in active state of the occupants and 18 °C in inactive state. The buildings are modelled in Modelica® to generate specific heat demand profiles for the buildings in the district using the TEASER modelling tool [47]. TEASER creates building models in Modelica® based on a few required input parameters such as building usage type, year of construction, class, or building height. TEASER offers the possibility to use the building types from [46] as an input to create building models making use of the typical building types. In addition, the fully refurbished building type is created in TEASER by setting the retrofit option presented in [46] as an additional input parameter.

Air conditioning (parameter (8)) is considered as an optional future trend. The thermal cooling demand profiles are calculated using TEASER, as well. For the calculation of the corresponding electrical load profiles, an air conditioning heat pump with a constant coefficient of performance of 3 is assumed, for simplicity. The temperature setpoint for air conditioning is chosen as 22 °C.

All the time series calculated by the PV simulation, LPG, and TEASER represent the base time series for the simulation. The co-simulation input time series required for the infrastructure simulations (see Section 3.5) are composed out of them according to the corresponding parameter set of the selected variation.

3.7. Grid operation

The heat demand in the district multi-energy system under consideration has to be covered independently from external heat supplies. For a flexible operation of the heat supply, the 50 m³ heat storage tank located in the CHP is used. Electrical power can be imported from or exported to the external grid. The primary goal of the grid operation is an efficient coverage of the heat demand. The heat demand is covered by the heat-driven operated gas turbine and in dependence on the simulated variation by additional power-to-heat. To keep the results comparable for all configurations, the grid operation must not be optimized for a specific configuration. This constraint is further discussed in Section 5.1.

Three operation modes (parameter (3)) are implemented. An operation without power-to-heat (3.1) serves as reference case. In the operation mode *peak shaving power-to-heat* (3.2), the power injected by the buildings exceeding 4.6 kW is converted into heat. In the *surplus power-to-heat* operation mode (3.3), all electrical surplus power is converted into heat. Power-to-heat is deactivated if the water temperature in the storage exceeds 90 °C on average.

The MGT is controlled with a PI controller in order to keep the temperature in the top layer of the heat storage tank at 75 °C. The MGT is turned off, as soon as the PI controller demands a thermal power output below 60 kW, as this is the minimum thermal output supported by the MGT. It is turned on again, as soon as the temperature in the top layer of the heat storage falls below 65 °C.

3.8. Key performance indicators

Sustainability science is an inter-disciplinary field considering interactions between nature and society [48]. Environmental challenges span from climate change over biodiversity loss and land use to water scarcity [49]. It is not always possible to identify one ideal solution [50]. Thus, the evaluation is performed using several key performance indicators, each representing another sustainability impact category.

Table 4 lists the key performance indicators calculated in the present contribution. As the decarbonization of the energy system is motivated by the mitigation of climate change, *Climate change impact* is selected as associated indicator and holds information on direct carbon dioxide emissions by the respective multi-energy system under investigation. Fuel consumption is covered by the indicator *Resource scarcity*, *Overall system efficiency* holds information on the heat generation within the investigated scenario. The *Degree of autarky* measures the energy import from the external power grid, last but not least, *Power quality* is a measure for the voltage not being exceeded 95% of the time, a technical indicator in the low-voltage distribution grid.

The selected key performance indicators represent the impact of the energy system operation on sustainability from a technical point of view. This result is an important part of a full life cycle assessment, where the impacts of all steps between mining and recycling need to be determined [51].

3.9. Limitations, assumptions, and simplifications

General statements and quantification of impacts are difficult to make. The traditional energy system differs from country to country and even within a country. On the building side, there are districts with similar buildings and districts with heterogeneous buildings. The presented simulation uses the same building type for all buildings within one scenario. However, the four building types represent a wide range of the German building stock and the corresponding heat demands.

The current work considers two different locations in Germany for the district energy system scenarios. In order to be able to make more general statements, meteorological test reference years considering climate input data would have been beneficial. Unfortunately, the required high temporal resolution impedes the usage of test reference years as input data. Therefore, data from the recent past is used as input. Note that fluctuations between several years and an increased temperature due to global warming are not considered in this contribution.

The same size of MGT is used for all variants. In some cases, the gas turbine is significantly oversized, which results in suboptimal operating behaviour and could be replaced in practice by a smaller model to improve efficiency. Similarly, the heat storage tank has a fixed size and is not dimensioned individually for each configuration.

The recorded shortwave irradiation time series, which serve as input data for the PV simulation, are only available for one point per location. For this reason, the PV generation is the same for all buildings. The resulting power at the busbars is however different, since the electrical load connected to the same busbar is individual.

Table 5

Overview of accumulated simulated annual heat demand of the whole district in all configurations without and including domestic hot water (DHW) preparation by district heating network.

| Location (10)	District (1)	Building type (2)	Accumulated annual heat demand in MWh	
			Without DHW	incl. DHW
Berlin-Adlershof	District 16	Old	697.8	766.2
Berlin-Adlershof	District 16	Medium	364.7	433.1
Berlin-Adlershof	District 16	Modern	194.2	262.6
Berlin-Adlershof	District 16	Refurbished	150.2	218.6
Berlin-Adlershof	District 48	Modern	586.0	786.3
Berlin-Adlershof	District 48	Refurbished	453.9	654.1
Eggenstein-Leopoldshafen	District 16	Old	668.2	736.4
Eggenstein-Leopoldshafen	District 16	Medium	348.2	416.4
Eggenstein-Leopoldshafen	District 16	Modern	187.2	255.5
Eggenstein-Leopoldshafen	District 16	Refurbished	145.3	213.5
Eggenstein-Leopoldshafen	District 48	Modern	569.6	769.3
Eggenstein-Leopoldshafen	District 48	Refurbished	443.3	643.1
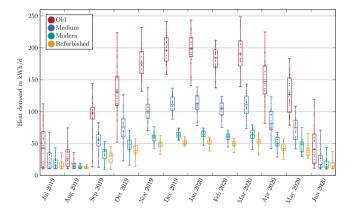
Fig. 4. Simulated heat demand incl. domestic hot water per day for an average over all buildings at Berlin.

The PV simulation considers no shading of modules. All PV systems are assumed to have the same configuration. As air conditioner a conservative device with an efficiency class F according to EU Standards [52] with a seasonal energy efficiency ratio of 3 is assumed.

4. Results

The results of the most significant simulations are presented and discussed in this section. The key performance indicators (see Table 4) of all conducted simulations are provided in the supplementary materials.

4.1. Building heat demand simulation

Parameters under consideration in this section:
(1) District
(2) Building type
(5) Domestic hot water supply
(10) Location

Fig. 4 depicts the simulated heat demand per day for District 16 (1.1) at Berlin (10.1). The depicted demand includes the heat used for space heating and for domestic hot water heating (5.1). From intuition, and also visible in the figure it is obvious that old buildings have a huge annual heat demand. Table 5 provides the corresponding numbers for the simulated conditions. The heat demand for old buildings amounts to 4.6 times of that of refurbished and 3.6 times that of modern buildings for the sum of buildings in the entire district. The two chosen locations differ by less than 5% in the calculated heat demand for respective configurations in both cases, with and without domestic hot water. For

the sake of simplicity, all results in the following sections refer to the location Berlin (10.1).
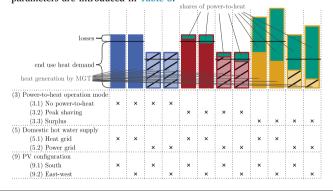
4.2. Power-to-heat

Parameters under consideration in this section:
(1) District
(2) Building type
(3) Power-to-heat operation mode
(4) Power-to-heat location
(5) Domestic hot water supply
(9) PV configuration

How to read the bar diagram in Fig. 5

For each combination of district size (1) and building type (2) a block of twelve bars is displayed. The twelve bars represent all possible combinations of the parameters (3), (5), (9) as displayed here. The parameters are introduced in Table 3.

In this section, the impact of the power-to-heat operation modes (no power-to-heat (3.1), peak shaving power-to-heat (3.2), surplus power-to-heat (3.3)) is evaluated. Note, that electrical domestic hot water heating is not considered as power-to-heat term in this context. Power-to-heat and the conventional heat generation by the gas turbine are closely related, since the share of power-to-heat influences the usage of the gas turbine for heat generation. The comparison is conducted for a natural gas fired MGT (6.1). Fig. 5 shows the annual heat generation by the natural gas fired MGT and by power-to-heat calculated in various configurations. Fig. 5(a) shows configurations with the distributed installation of power-to-heat (4.1) and Fig. 5(b) configurations with the central power-to-heat installation located in the CHP (4.2). We vary the parameters (3) power-to-heat operation mode (reference case *no power-to-heat* (3.1) [in blue], *peak shaving* (3.2) [in red], *surplus*

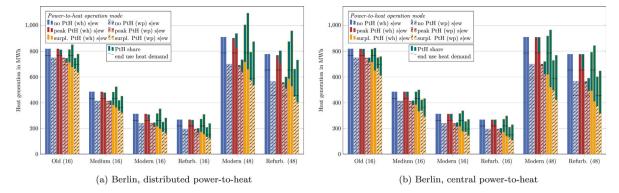(a) Berlin, distributed power-to-heat   (b) Berlin, central power-to-heat

Fig. 5. Annual heat generation by the MGT and by distributed (Subfigure (a)) and central (Subfigure (b)) power-to-heat (green) over the considered duration of one year at Berlin. For each combination of building type and district size, the power-to-heat operation mode *no PtH* as reference case without power-to-heat, *peak PtH* where peak shaving of PV injection is used for power-to-heat, and *surpl. PtH* where all surplus power from PV is converted into heat are simulated. In each case the heat generation by the MGT and by power-to-heat is displayed for domestic hot water heating by district heating network (wh), and by power grid (wp). Of every pair of bars, each left bar shows the result for the PV oriented south (s), while the right bar shows the results for the PV on the east and the west roofs (ew).
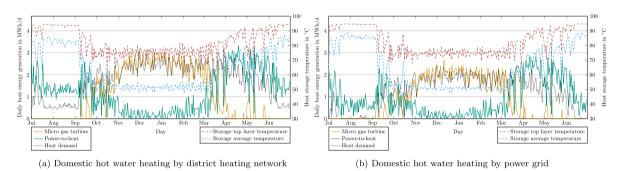

(a) Domestic hot water heating by district heating network   (b) Domestic hot water heating by power grid

Fig. 6. Daily heat production by MGT (orange) and central power-to-heat (green) in District 48 in surplus power-to-heat operation mode at Berlin for east–west oriented PV. The state of charge of the heat storage tank is indicated by the daily average temperature of the top layer (dashed red line, limited to 95 °C) and the average temperature of all layers (dashed cyan line, limited to 90 °C). The dotted black line represents the heat demand.

(3.3) [in orange]), (5) domestic hot water supply (*by heat grid* (5.1) [fully coloured bars], *by power grid* (5.2) [hatched bars]), and (9) PV-orientation (*south oriented PV roofs* (9.1) [left bar of a pair], *east and west oriented PV roofs* (9.2) [right bar of a pair]). This results in 12 combinations, see the explanation box. Additionally we marked the shares of the end use heat demand and losses by a black bar. The green areas depict the share of power-to-heat. On the x-axes each group of 12 bars is assigned to the chosen district size (1) and building type (2).

For the power-to-heat configurations (3.2) and (3.3), i.e. red and orange bars, a reduction in heat supplied by the MGT (lower height of bars subtracting the green area) is expected compared to the reference case (3.1) [in blue]. This is achieved in all respective configurations. However, the total heat generation (sum of MGT and power-to-heat) is particularly in configurations with distributed power-to-heat (4.1) and a high share of power-to-heat [orange–green bars in Fig. 5(a)] significantly higher than in the reference case without power-to-heat (4.1) [blue bars]. This results from the higher heat transport activity in the distributed power-to-heat configuration (4.1). The heat needs to be transported from the distributed direct-electric heaters to the central heat storage tank and holds therefore greater losses due to transport in comparison to the central power-to-heat configuration (4.2).

The heat losses accompanied by power-to-heat in comparison to the reference case are exemplarily quantified for the configurations with refurbished buildings (2.4) in District 48 (1.2) [right 12 bar block]. Losses accompanied with power-to-heat are the share of the green power-to-heat areas in Fig. 5 higher than the associated [blue] reference case bar. In the distributed power-to-heat configuration (4.1) (see Fig. 5(a)) in the surplus power-to-heat operation mode (3.3), the share of power-to-heat that is lost in comparison to the associated reference scenario is 34.2% for domestic hot water heating by district heating network (5.1) and south oriented PV (9.1) (42.3% for east and

west oriented PV (9.2)). For domestic hot water heating by the power grid (5.2) and south oriented PV (9.1), the losses are 45.0% (50.9% for east and west oriented PV (9.2), respectively).

In contrast, the corresponding losses attributed to central power-to-heat (4.2) (Fig. 5(b)) are only 5.4% (5.1, 9.1), 15.5% (5.1, 9.2), 16.2% (5.2, 9.1), and 24.6% (5.2, 9.2).

Noteworthy in this context is an unexpected slightly reduced total heat generation for cases in peak shaving operation mode (3.2) for distributed power-to-heat (4.1) [red–green bars in Fig. 5(a)]. The reason is the dominating effect of power-to-heat conversion and heat demand in the buildings at the same time with no need for heat transport via the pipes. The corresponding diagrams for the location Eggenstein-Leopoldshafen (10.2) are provided in Supplementary Figure 2. There, the effects mentioned in the previous paragraphs occur as well. The absolute values differ slightly due to the different heat demand.

We compare the daily heat production by a gas turbine and by power-to-heat for the two cases domestic hot water heating by district heating network (5.1) in Fig. 6(a) and domestic hot water heating by power grid (5.2) in Fig. 6(b). This is done for the above discussed configuration District 48 (1.2), Refurbished buildings (2.4), Central power-to-heat (4.2), East–west oriented PV (9.2). The heat storage tank average temperature is a measure for the state of charge. The temperature indicates that the storage operates at a high level in summer and, thus, limits the potential for power-to-heat. For domestic hot water heating by electricity grid (Fig. 6(b)), there is hardly any heat demand in summer and the stored energy remains mostly unused. The relatively high difference between the heat generation and heat demand in summer is remarkable. The reason is a minimal circulation mass flow in the pipe network to avoid stagnant fluid. If domestic hot water is heated by district heating network (Fig. 6(a)), the complete heat demand for domestic hot water is covered by power-to-heat in
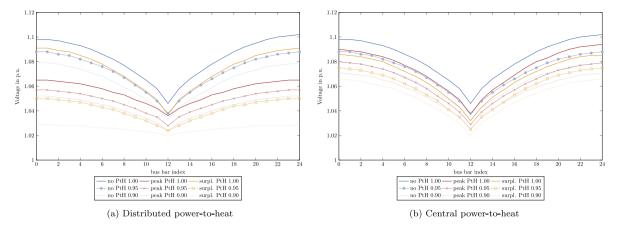
(a) Distributed power-to-heat

(b) Central power-to-heat

Fig. 7. Voltage distributions for District 48, Refurbished buildings, and East–west PV between May 28th, 2020 and June 3rd, 2020 based on 10 min average. Each line displays the voltages that are not exceeded in the associated share of time. The power-to-heat operation modes peak shaving and surplus yield a significant voltage reduction for distributed power-to-heat (Subfigure (a)). Supplementary Figure 3 depicts the voltage distributions in 0.01 granularity.
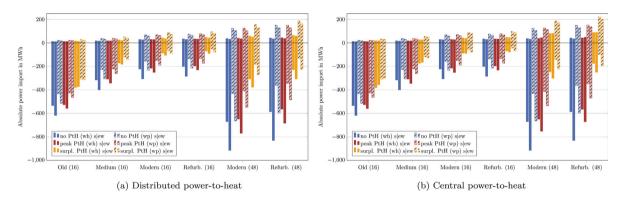

(a) Distributed power-to-heat

(b) Central power-to-heat

Fig. 8. Annual absolute power import (positive) and export (negative). Surplus power generated by the CHP or PV is exported to the external grid. The bars are displayed in analogy to Fig. 5. Expectable changes caused by future trends such as dissemination of battery electric vehicles and air conditioning are provided in Supplementary Figure 5.

summer. Significant losses beyond the already known circulation flow hardly occur.

In order to provide flexibility during all seasons, heat distribution via the district heating network is required in all seasons. Especially June to August are challenging, since the space heating demand is very low in these months (see Fig. 6(b)). To exploit the large generation in these high insolation months, it is necessary to provide the heat for domestic hot water via the district heating network (5.1) and, thus, profit from the flexibility of heat storage in combination with power-to-heat.

4.3. Distribution power grid

> *Parameters under consideration in this section:*
> (3) Power-to-heat operation mode
> (4) Power-to-heat location
> (11) CHP connection

A high share of fluctuating energy sources in the distribution grid is challenging for the power quality [6]. A high PV feed-in can cause high voltages at the line ends and a high line loading. According to EN 50160 [53], the voltage averaged over 10 min shall stay within the voltage band limits of 0.9 p.u. and 1.1 p.u. for 95% of the time within one week. Therefore, increasing PV feed-in on the district level is a risk for the voltage stability. One measure tackling the problem with line overloading and overvoltage is feed-in curtailment to 70% of the peak power. Consumption close to the power generation can lower the voltage and thus prevent unnecessary cut-off.

Fig. 7 shows the voltage distribution in the electricity grid for District 48 (1.2) with east and west oriented rooftop PV (9.2) and domestic hot water heating by the district heating network (5.1) between May 28th 2020 and June 3rd 2020, the week with the highest PV generation in the considered time span. The 1.00 curve shows the overall maximum values, the 0.95 curve the voltage that is not exceeded 95% of time, the 0.90 curve the voltage that is not exceeded 90% of time. Power-to-heat in peak shaving (3.2) or surplus (3.3) operation mode reduces the voltage. In both operation modes, the 0.95 curve is significantly reduced for distributed power-to-heat (Fig. 7(a)) compared to central power-to-heat (Fig. 7(b)). Despite power-to-heat positioning near to the PV modules in the distributed power-to-heat configuration (4.1), the voltage is not reduced to a nearly constant value, since the heat storage capacity is limited and power-to-heat needs to be disabled if this limit is reached. Thus, the extent of thermal demand must be taken into consideration if the capability to reduce the voltage using distributed power-to-heat is investigated. Using a peak shaving operation mode can sustain the storage capacity for PV feed-in peaks. For this reason, the orange 1.00 surplus power-to-heat curve is higher than the corresponding red peak shaving power-to-heat curve in Fig. 7(a).

Apart from distributed power-to-heat units, the voltage could even be reduced in a central configuration, if the power-to-heat unit would be positioned further away from the transformer as marked in light grey in Fig. 1. The voltage distributions for a central power-to-heat configuration compared to power-to-heat located near the transformer (11.1) and inside the electrical grid (11.2) are depicted in Supplementary Figure 4. However, changing the position of the CHP is barely possible in already existing habitated districts due to limited flexibility in the use of space.
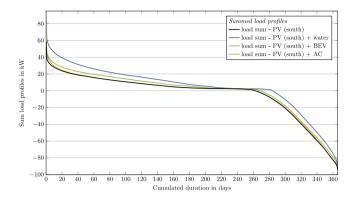
Fig. 9. Electrical residual load duration curves for the District 16 case at Berlin. The summed load profiles over all 16 buildings are displayed in the base form and with additional consumers for the scenarios with electric domestic hot water heating, air conditioning (building type *Medium*), and BEVs. The PV generation for south oriented modules is already subtracted from the summed load profiles.

All of the considered configurations meet the voltage band requirement. Nevertheless, slightly larger line lengths or district sizes may violate the voltage requirement.

The power exchange with the external grid is displayed in Fig. 8. The energy generated by cogeneration of heat and power dominates the power export. Configurations with low power export show an increased import demand due to less cogeneration.

4.4. Future trends: Dissemination of battery electric vehicles and air conditioning

Parameters under consideration in this section:
(7) Mobility
(8) Air conditioning
(10) Location

The electrical demand increases in future due to electrification of mobility and dissemination of air conditioning. The residual load without any power-to-heat for both future trends is displayed in Fig. 9. Charging at home cannot be covered sufficiently by rooftop PV and needs additional imported power or power generated by the heat-driven operated MGT. The annual energy demand for charging is 1.485 MWh on average per BEV. As visible in Supplementary Figure 5, the additional load by BEVs charging at home is covered by local generation in a high share (compare the export with and without BEV mobility) in cases with no (3.1), or peak shaving (3.2) power-to-heat. In these cases, the electrical power generated by the CHP is more frequently available at night than in the surplus power-to-heat operation mode (3.3) with generally less MGT operation. Air conditioning seems to play a subordinate role as could already be anticipated from its low additional load visible in Fig. 9.

The average annual energy demand for air conditioning is 242 kWh for a refurbished building (2.4) at Berlin (10.1) and 155 kWh at Eggenstein-Leopoldshafen (10.2). Drawing conclusions about future scenarios need to be done carefully, since the climate conditions must be considered. The climate conditions will change in the future and already minor changes could cause a more frequent exceeding of the selected 22 °C threshold by the room temperature compared to the simulation using past weather recordings (see limitations in Section 3.9).

4.5. Carbon emissions and fuel demand

Parameters under consideration in this section:
(1) District
(2) Building type
(3) Power-to-heat operation mode
(4) Power-to-heat location
(5) Domestic hot water supply
(6) Micro gas turbine fuel
(9) PV configuration

Cogeneration of heat and power by an MGT is already an efficient form of power generation. Nevertheless, burning fossil fuels is accompanied by carbon emissions.

Fig. 10 shows the carbon dioxide emissions associated with the configurations already introduced in Figs. 5 and 8 for natural gas (6.1). A significant reduction of carbon dioxide emissions by 46% is achieved for District 48 (1.2) with central power-to-heat (4.2) in surplus operation mode (3.3), refurbished buildings (2.4), domestic hot water heating by district heating network (5.1), and east–west oriented PV (9.2) (compare the orange, shaded bar on the far right with the associated red, shaded bar of the reference case without power-to-heat in Fig. 10). The specific emissions related to the produced heat are about 408 g/kWh (thermal) and nearly the same in all configurations. Note that this value does not take into account the simultaneous electricity generation and is thus high compared to common gas boilers. More details on emissions in relation to the demand are given in Supplementary Figure 6. All configurations with two PV equipped roof sides (east–west) and power-to-heat in operation emit less carbon dioxide than the corresponding configurations with only one equipped roof side (south). The demand for natural gas is strongly related to the carbon emissions. The resulting fuel demand for all simulated configurations is provided in the supplementary materials.
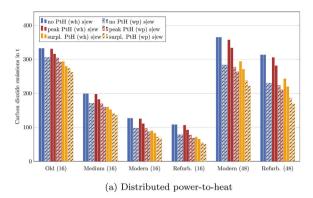
4.6. Energy system performance evaluation

Parameters under consideration in this section:
(1) District
(2) Building type
(3) Power-to-heat operation mode
(4) Power-to-heat location
(5) Domestic hot water supply
(9) PV configuration

Fig. 11 shows the performance of the considered energy system as radar charts of the key performance indicators defined in Section 3.8 for District 16 (1.1). Figs. 11(a) to 11(d) show the impact on the key performance indicators for all building types (2) and power-to-heat operation modes (3). The magnitude is normalized to the maximum indicator amplitude which is 332.2 t for indicator CO2, 121.3 t for fuel consumption FC, 851.1 MWh for heat generation HG, 80.8 MWh for energy import EI, 617.9 MWh for energy export EE. U95 is set to 0.033 p.u. related to the overshoot of 1 p.u. in the annual average.

The indicators in the categories climate change impact (CO2) and resource scarcity (FC) have a nearly linear relationship due to the MGT being both the only emitter and the only fuel consumer in this scenario. The impact of the buildings' thermal insulation (2) on FC and CO2 is enormous (compare old and refurbished buildings). Refurbishing has no significant negative impact on other indicators apart from decreased local electricity generation by reduced cogeneration. Power-to-heat supplied by local PV has in contrast a significantly lower impact. However, with power-to-heat in surplus operation mode, CO2 and FC are already reduced by about 12% for old buildings (2.1) and south
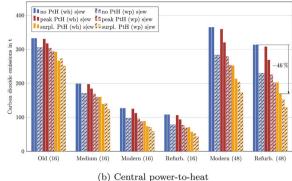
(a) Distributed power-to-heat

(b) Central power-to-heat

Fig. 10. Annual carbon dioxide emitted by the gas turbine for distributed and central power-to-heat at Berlin. The bars are displayed in analogy to Fig. 5. Emissions relative to the demand are provided in Supplementary Figure 6.

Table 6

Annual energy demand to reach carbon neutrality by replacing natural gas with SNG in surplus operation mode for central power-to-heat, refurbished buildings in District 48. For the production of 1 kg SNG an energy demand of 25 kWh is assumed.

Domestic hot water heating (5)	PV orientation (9)	SNG demand t	Energy for SNG GWh	Energy export GWh	Difference GWh
District heating network (5.1)	South (9.1)	73.8	1.845	0.175	1.670
District heating network (5.1)	East–west (9.2)	61.7	1.543	0.250	1.293
Power grid (5.2)	South (9.1)	55.9	1.398	0.100	1.298
Power grid (5.2)	East–west (9.2)	47.4	1.185	0.198	0.987

oriented PV (9.1). The peak shaving operation mode for power-to-heat (3.2) makes only a significant difference for the east–west PV configuration (9.2) where the power exceeds the threshold more often. The east–west PV configuration compared to the south configuration saves emissions for power-to-heat in peak shaving and surplus operation mode. The emission reduction potential is particularly pronounced in the case of unrenovated old buildings. The electrical energy export (EE) is composed of energy generated by PV and the one from MGT cogeneration that is not consumed by local consumers or converted into heat. Thus, a high share of heat generation by the MGT causes high EE. A frequent operation of the MGT influences the voltage indicator U95 as well, but the considerable reduction by surplus power-to-heat (3.3) is clear. Apart from that effect, the impact on the electrical energy import EI is nearly inverted in relation to the other indicators. The reason for this is also the cogeneration. A more frequent operation of the MGT can cover the local electrical demand more often.

The district size has a significant influence on voltage distribution and autarky (compare Figs. 11(d) to 11(e)). While the longer line length in District 48 (1.2) increases the U95 indicator, the power import EI is significantly reduced relative to the number of buildings. The main reasons are the slightly higher thermal losses in the larger pipe network (see Section 4.2) and thus an increased cogeneration of heat and power in the CHP which accounts as a power source within the district. All corresponding diagrams for District 48 are provided in Supplementary Figure 7.

Fig. 11(f) shows configurations with electrical heated domestic hot water for distributed power-to-heat and east–west oriented PV (9.2). Compared to the cases with domestic hot water by district heating (Fig. 11(d)), the heat generation and the impact on climate change and fuel demand is reduced, but the energy import is increased very clearly. Note that this power import can cause emissions outside the district boundaries. Particularly in the summer time when the heat demand for space heating is very low, domestic hot water heated by the district heating network (5.1) can help to achieve a high self-consumption of PV energy using heat storage and thereby increases the power-to-heat potential and thus reduces U95.

4.7. Decarbonization of the remaining fuel demand with synthetic fuels

Parameters under consideration in this section:
(5) Domestic hot water supply
(6) Micro gas turbine fuel
(9) PV configuration

Replacing the fossil fuel with synthetic fuels is an easy measure to implement, as it only affects the CHP. The additional energy demand for the decarbonization of natural gas using synthetic natural gas (SNG) and the energy demand for hydrogen production are calculated. Hydrogen as a means for energy storage can be converted into electricity and heat with an overall efficiency of more than 90% with respect to its energy content. However, when electricity transmission, electrolysis efficiency and hydrogen transport are taken into account, about 50% of the energy is lost in the process of providing hydrogen [54].

In Table 6, the annual electrical energy demand for a green production of SNG and in Table 7 for hydrogen is shown. An energy demand of 25 kWh/kg for SNG and 74 kWh/kg for hydrogen (including transmission, electrolysis, and transport losses) is assumed (see [54]). Even in the most beneficial configuration, there is a need for nearly 1 GWh in addition for SNG and 1.2 GWh for hydrogen to the surplus power assigned for power export. East–west PV configurations with modules on both sides of the roof reduce the demand for fuel considerably. Fuel demand is also lower for domestic hot water heated by power grid, but the associated higher electricity import (see Section 4.6) requires considerations of energy generation across district borders.

The enormous additional energy demand required for the production of synthetic fuels needs a trade-off between additional energy generation capacity outside and efforts for further measures inside the district.

5. Discussion

The present contribution provides a multiplicity of parameter sets in order to capture the relation of indicator magnitudes in different impact
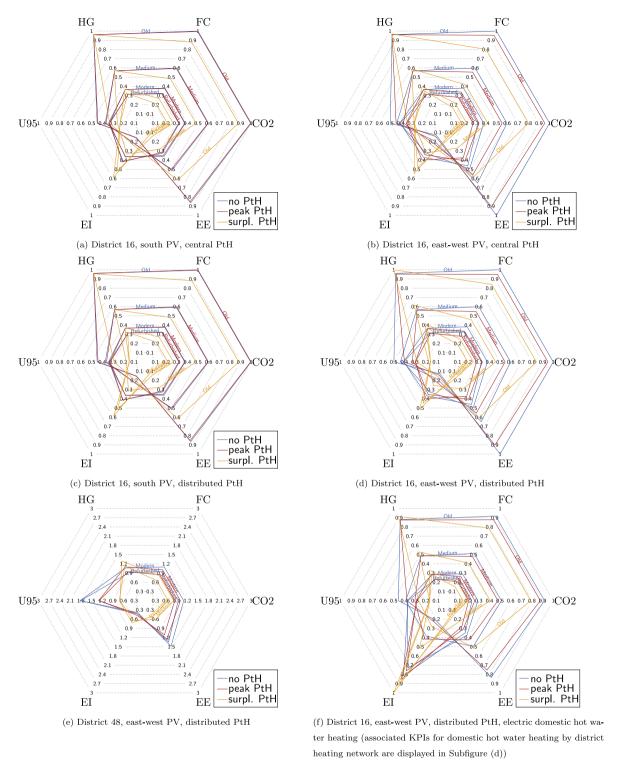
(a) District 16, south PV, central PtH

(b) District 16, east-west PV, central PtH

(c) District 16, south PV, distributed PtH

(d) District 16, east-west PV, distributed PtH

(e) District 48, east-west PV, distributed PtH

(f) District 16, east-west PV, distributed PtH, electric domestic hot water heating (associated KPIs for domestic hot water heating by district heating network are displayed in Subfigure (d))

Fig. 11. Key performance indicators CO_2 emissions (CO2), fuel consumption (FC), heat generation (HG), electrical energy import (EI), electrical energy export (EE), line end voltage (U95) from Table 4 for selected configurations. The values are normalized to the associated maximum occurring value.

Table 7

Annual energy demand to reach carbon neutrality by gas turbine operation with hydrogen in surplus operation mode for central power-to-heat, refurbished buildings in District 48. For the production of 1 kg hydrogen an energy demand of 74 kWh is assumed.

Domestic hot water heating (5)	PV orientation (9)	H₂ demand t	Energy for H₂ GWh	Energy export GWh	Difference GWh
District heating network (5.1)	South (9.1)	30.6	2.264	0.179	2.085
District heating network (5.1)	East–west (9.2)	25.6	1.894	0.255	1.639
Power grid (5.2)	South (9.1)	23.2	1.717	0.103	1.614
Power grid (5.2)	East–west (9.2)	19.2	1.421	0.202	1.219

categories. With this, it is possible to assess the impact of design or development decisions for district multi-energy systems.

5.1. Implications for the further development

In the holistic consideration of all analysed district configurations, measures, and future trends, a reduction of the heat demand caused by modernization of buildings in combination with rooftop PV installation promises the highest decarbonization impact. The combination allows for achieving a considerable share of renewable heat generation using power-to-heat and heat storage. However, interdependencies complicate general statements. Power-to-heat conversion enables the flexibility of heat storage to be used for locally generated PV energy. A high PV feed-in increases the voltage in the low-voltage distribution grid. This undesirable effect can be mitigated by distributing the power-to-heat conversion boilers in the district. This in turn increases the heat flow and implies higher losses. Converting as much PV energy into heat as possible is most effective for reducing fossil fuels in winter. In summer, large PV installations might undergo curtailment as that much heat generation is not needed. In contrast, operating power-to-heat in a peak-shaving mode reduces the peak voltages more reliably but demands more fuel. An important factor to enhance the power-to-heat capacity in summer is to heat domestic hot water by the district heating network.

The present contribution operates the system in a comparable manner for different configurations. Once the final design is established, more specific circumstances offer operational optimization potential. A case-specific optimized operation of the MGT and power-to-heat considering the local circumstances may enhance the system performance. This operation strategy needs to distinguish the seasons in order to find a trade-off between peak shaving and surplus operation mode in order to increase the sustainability and sustain a feasible voltage level. This includes to consider an appropriate time horizon for the heat storage and calculate forecasts for heat demand and PV generation.

The dissemination of battery electric vehicles used for inner-city routes benefits from the cogeneration of the CHP. The impact of an extensive usage of battery electric vehicles for long distances is subject of further research. The still high amount of exported energy promises further self-consumption potential. However, a detailed analysis is required for a reliable statement.

Replacing fossil fuels with synthetic fuels can be implemented centrally in the CHP without measures in the buildings. However, the enormous additional energy demand needed for the production of synthetic fuels requires a trade-off between additional energy generation capacity outside and efforts for further measures within the district.

5.2. Impact of extensive PV deployment

An extensive PV equipment of the available roofs is assumed in this contribution, since PV is an energy source that is available in residential areas close to the consumers. Assessments in terms of sustainability, feasibility, and economy can vary due to geographical circumstances. Today's glass-backsheet PV modules produced in the EU possess a global warming potential (GWP100) of $480\,kg\,CO_2$ equivalents per kW peak power [55]. These emissions are already saved with the presented 46% emission reduction by power-to-heat in surplus operation mode in 2.2a. The levelized cost of energy of PV on small roofs was below 0.11€ per kWh in 2021, on large roofs below 0.11€ per kWh [56], which is even competitive with gas prices.

A high PV feed-in on sunny days can cause issues in the low-voltage distribution grids which are avoided by curtailment. District multi-energy systems help to unlock the flexibility of heat for the PV generation. If the space available for PV is limited anyway like in urban areas, a highly efficient utilization of the available energy is required. A high degree of cross-sectoral autarky should be the goal in order to relieve the power grid and reduce the tremendous demand for carbon

neutral fuels. The expected drastic increase in deployment of rooftop PV [57,58] will not only challenge the load of the distribution power grids [6] but also the supply capacity for PV system components (flat glass, silver, aluminium, electronics etc.) [59].

5.3. Comparison with related studies

The studies [14–17] presented in Section 2.2 use a comparable system configuration to the present one.

Salpakari et al. [14] achieve over 80% heat generation with power-to-heat for the years 2013 to 2015. The most comparable case in the present contribution is central power-to-heat (4.2) in surplus operation mode (3.3). We achieve between 21% for old buildings (variation ID 1192 in the supplementary materials) and 53% for refurbished buildings (variation ID 1198). The main differences to Salpakari et al. are the power-to-heat technology and the renewable sources. Salpakari et al. [14] use heat pumps with a coefficient of performance of 3 in a magnitude of 50% of the nominal renewable power and electric boilers for the rest. We use only the cheaper but less efficient electric boilers. The renewable energy sources used in [14] are mainly 500 offshore wind turbines near to the coast of Helsinki and a little share of PV in summer while we consider only PV. The very different geographical circumstances show that it is not possible to find general solutions and there is a need to either consider a specific configuration for a selected location or to consider a broad range of possible configurations.

The potential of power-to-heat in districts to reduce the negative residual load on a national scale is determined by Schweiger et al. [16] and Böttger et al. [17]. Schweiger et al. [16] calculate 11% for Sweden in the year 2050 and Böttger et al. [17] 9% for Germany in the year 2030. The high differences compared to the closed area considerations in this contribution and in [14] show the huge demand to use the potential of locally available energy sources in order to decarbonize the heating sector. However, PV-dominated district multi-energy systems can expect to receive renewable energy from the national scale in windy times.

Widl et al. [15] compare different operation strategies for power-to-heat. The buildings are equipped with 11.9 kW peak power PV modules on average. Although the exact roof configuration has some influence, it is of a similar magnitude to the east–west configuration (9.2) with 6.8 kW peak power on each roof side. The heat demand of the buildings in [15] lies between the heat demand of the medium (2.2) and the old (2.1) building type in this contribution. Power-to-heat reduces the demand for imported heat in [15] between 14.5% for an economical operation and 25.6% for an eco-friendly operation. We achieve a reduction of heat generated by the MGT by 20.9% for the old building type in surplus operation mode at Eggenstein-Leopoldshafen (distance to [15] less than 140 km) and 31.5% for medium type buildings. This result is comparable to the ecofriendly operation in [15] and supports their result.

5.4. Strengths and weakness of the method

The results presented here and in the supplementary materials allow a comparison of measures in many combinations for the expansion of existing district multi-energy systems. In order to reach a certain degree of comparability, we have chosen to simulate a standard district [24], see Section 3.2. As Saelens et al. [24] notice, the small district with 16 buildings needs to be scaled in order to represent typical district sizes. Due to the maximal thermal power of the MGT of 180 kW, the results can be related to small districts but not on a city scale. The same MGT is used for all configurations. On the one hand, this provides good comparability, but on the other hand it does not exploit the potential for an optimally dimensioned MGT. As the simulated district multi-energy system is a benchmark that is not available in reality, the validation needs to be performed on components level. The grid models are modelled using base components (e.g. lines and pipes) of the

established libraries AixLib and Pandapower (see Section 3.5.1). The gas turbine model is verified by measurements (see Section 3.5.2) and the electrical load profiles using plausibility checks and comparisons of annual energy consumption and load duration curves [44]. The results of the PV and heat demand profile simulations strongly depend on the weather data input.

We have taken into account the diversity of the individual districts by means of parameter sets (see Section 3.1) that describe different construction measures, structural conditions, and future trends. To the best of our knowledge, the extent of 3840 simulated configurations in a high resolution has not been achieved by previous works in this context. Nevertheless, the number of simulated parameter values in each configuration parameter is limited. The configurations for PV, building types, and power-to-heat are selected in order to show the range of the simulation results and the potential for the single measures. Existing buildings in a real district are usually very heterogeneously equipped and their results might be in between the associated simulated homogeneous configurations.

Modelling a specific neighbourhood with differently equipped buildings achieves a very high significance of the results under the given conditions, but the diversity of neighbourhoods lowers the generalizability. The simulation results for the same setups and within the same considered time span at two different locations are very similar. Significantly differing climatic conditions like in other geographical regions, variability between the years, or those resulting from extensive global warming are not covered in this contribution.

The availability of weather data is crucial as they are input data for the load simulations. The PV simulation in particular requires short-wave irradiation data in a high temporal resolution (see Section 3.4). Unfortunately, it was not possible to receive all required measurements without gaps in a sufficiently high temporal resolution for both locations. Hence, we use high-resolution meteorological recordings from research weather stations and complement gaps and missing quantities from other sources. The present simulation uses measurements of the thermal radiation for Eggenstein-Leopoldshafen and ERA5 forecast data [40] for Berlin. We suppose a slight underestimation and, thus, a slight overestimation of the heat demand in the urban environment of Berlin.

The time span from July 2019 till June 2020 is selected for weather data availability reasons. Multi-year outlooks could achieve an increased long-term representativeness, but limited availability of long-term recordings without gaps impede that.

Unfortunately, the temporal resolution of the weather data captured at Berlin is reduced from $1\,\mathrm{min}$ to $10\,\mathrm{min}$ between January 2020 and June 2020 due to a logging issue. This issue mainly influences the PV simulation and subsequently also the power grid simulation. An estimation of the issue's impact is difficult, since the error magnitude depends on the sky conditions and mainly affects the power peaks (see [60]). This should affect possible overshoots of the power-to-heat threshold in the peak shaving operation mode (3.2) and the voltage indicator U95. Since the differences in the respective indicators between the two locations (10) are low, the temporary reduction of the Berlin weather data's temporal resolution is not classified as a major issue.

5.5. Future research potential

The investigated multi-energy system is considered within the district's boundaries. The interaction with the neighbourhood and environment is represented by power imports and exports as well as emissions and fuel consumption. In the present contribution, the accounting of power import and power export does not take the availability of other renewable energy sources like wind or hydropower in the wider surroundings into account. At the time of low availability of renewables, other districts in the neighbourhood with electrical heating technologies may benefit from the cogeneration of heat and power.

In order to increase the efficiency of the district heating network, various design adjustments could be considered in further studies. In the considered distributed power-to-heat configuration (4.1), the heat losses in the return pipes are relatively high while the heat is transported to the central heat storage tank. The electricity converted into heat could be stored on-site by installing decentralized buffer storage tanks within the buildings.

Heat pumps can achieve a higher supply efficiency which depends on the temperature level of the system and are already used for power-to-heat in a district heating network by Salpakari et al. [14]. However, heat pump systems are more complex and expensive than direct electric heaters. Therefore, the higher operation efficiency must be weighed against higher investment by considering the annual power-to-heat operation.

In this contribution, the immediate consumption of locally generated PV electricity is assumed. An additional consideration of battery storage would cause conflicting objectives which decrease the assignability of occurring impacts. Hence, a supplementation by demand side response, or battery storage which would increase self-consumption and, thus, autarky is not considered. However, compared to the roughly estimated heat storage capacity of $2.3\,\mathrm{MWh}$ of the $50\,\mathrm{m}^3$ heat storage tank, today's common battery storage capacities would only account for a fraction. Shared battery storage options for the district could be a resource-saving approach, but operation for the good of community is challenging since the peoples's attitudes differ in different societies [61]. In the case with already available battery electric vehicles, bidirectional vehicle-to-grid concepts [62] can provide a resource efficient battery storage, but the operation requires smart grid communication infrastructure. A deeper investigation in this context remains a research topic.

The low heat demand and high PV injection in summer limit the capability for self-consumption of surplus PV. Depending on local circumstances seasonal thermal energy storage can provide long-term storage. Seasonal thermal energy storage is beneficial when there are several weeks or months between the occurrence of energy surplus and energy demand. In general, seasonal heat storage in district applications requires much larger storage capacities (few hundred MWh to GWh) than buffering heat for a couple of days. The geographic requirements need obviously very site specific analyses. In the considered district, a seasonal thermal energy storage would displace the MGT and thus reduce electricity generation. The heat pump would increase the electricity consumption. For a quantification and evaluation of these effects, the integration of a seasonal storage into the district multi-energy system model is required.

Furthermore, locally available prioritized heat sources like waste heat (see [63,64]) reduce the fuel demand, but can also reduce the power-to-heat potential as shown by Schweiger et al. [16] and need therefore to be integrated in the simulation.

Finally, the convenience of the simulated loads and generation and thus also weather input data is of utmost importance. Hence, future works should carefully select the data sources in order to cover a suitable observation time span and get feasible load and generation profiles. A detailed examination of data sources and data syntheses for suitability could facilitate this selection.

6. Conclusion

The presented simulation and comparative analysis gives an overview on the effect of different measures for existing multi-energy systems to reach more sustainability. PV as a renewable energy source in residential areas is considered in terms of a high exploitation to cover the demands for electricity, heat, and domestic hot water supply.

Highly detailed simulation models are performed to achieve a beneficial integration of PV in a cross-linked interaction of the district heating network and the power grid with power-to-heat.

In the holistic consideration of all analysed district configurations, measures, and future trends, a low heat demand caused by modern buildings or refurbishment of existing buildings in combination with high PV equipment promises the highest decarbonization impact and enables a considerable share of renewable heat generation using power-to-heat and heat storage. Small measures like power-to-heat, that can be implemented faster than building refurbishment, already contribute to the reduction of emissions, but further efforts remain towards net-zero.

Supplementing the existing fossil heat generation with power-to-heat reduces the carbon dioxide emissions by up to 46%. Power-to-heat is a cross-sectoral link between the power grid and the district heating network and unlocks the heat flexibility to the power side. A distributed power-to-heat configuration allows to reduce the voltage in the distribution grid significantly when the PV feed-in is high. This, in turn, is associated with higher distribution losses on the heat side. The power-to-heat capacity is limited by the heat demand. Heating the domestic hot water by district heating network is identified as an important measure in order to use the heat flexibility in the months with a high PV generation.

In order to fully decarbonize the heat supply, synthetic fuels can be used instead of natural gas. To achieve climate neutrality via using synthetic fuels, at least 987 MWh of additional electrical energy per year is required for the 48 buildings district.

Individual conditions in district multi-energy systems need individual measures in order to achieve a sustainable energy supply. This contribution shows the effect of the single steps towards this goal for a multiplicity of configurations.

CRediT authorship contribution statement

Anselm Erdmann: Conceptualization, Methodology, Software, Writing – original draft. **Anna Marcellan:** Conceptualization, Methodology, Writing – original draft. **Jan Stock:** Methodology, Writing – original draft. **David Neuroth:** Methodology, Writing – original draft. **Christian Utama:** Methodology, Software, Writing – original draft. **Michael Suriyah:** Conceptualization, Writing – original draft. **Sina Steinle:** Methodology, Writing – original draft. **Felicitas Müller:** Methodology, Writing – original draft, Writing – review & editing, Funding acquisition. **Dominik Hering:** Conceptualization, Methodology, Writing – review & editing. **Henning Francke:** Conceptualization, Writing – original draft, Writing – review & editing. **Sascha Gritzbach:** Conceptualization, Writing – original draft. **Martin Henke:** Conceptualization, Writing – original draft. **Noah Pflugradt:** Conceptualization. **Hüseyin Çakmak:** Writing – review & editing. **Leander Kotzur:** Funding acquisition. **Detlef Stolten:** Funding acquisition. **Thomas Leibfried:** Funding acquisition. **Dirk Müller:** Writing – review & editing, Funding acquisition. **Rutger Schlatmann:** Conceptualization, Funding acquisition. **André Xhonneux:** Writing – review & editing, Funding acquisition. **Veit Hagenmeyer:** Conceptualization, Writing – review & editing, Funding acquisition. **Carolin Ulbrich:** Conceptualization, Writing – original draft, Funding acquisition.

Declaration of competing interest

The authors declare that they have no known competing financial interests or personal relationships that could have appeared to influence the work reported in this paper.

Data availability

Data will be made available on request.

Appendix A. Supplementary data

Supplementary material related to this article can be found online at https://doi.org/10.1016/j.enconman.2023.117226.

References

[1] Li Yu, Rezgui Yacine, Zhu Hanxing. District heating and cooling optimization and enhancement – Towards integration of renewables, storage and smart grid. Renew Sustain Energy Rev 2017;72:281–94.

[2] Lund Henrik, Østergaard Poul Alberg, Chang Miguel, Werner Sven, Svendsen Svend, Sorknæs Peter, Thorsen Jan Eric, Hvelplund Frede, Mortensen Bent Ole Gram, Mathiesen Brian Vad, Bojesen Carsten, Duic Neven, Zhang Xiliang, Möller Bernd. The status of 4th generation district heating: Research and results. Energy 2018;164:147–59.

[3] Kleinertz Britta, Gruber Katharina. District heating supply transformation – strategies, measures, and status quo of network operators' transformation phase. Energy 2022;239:122059.

[4] European Commission. A clean planet for all a European strategic long-term vision for a prosperous, modern, competitive and climate neutral economy. 2018.

[5] Victoria Marta, Zhu Kun, Brown Tom, Andresen Gorm B, Greiner Martin. Early decarbonisation of the European energy system pays off. Nature Commun 2020;11(1).

[6] Gupta Ruchi, Pena-Bello Alejandro, Streicher Kai Nino, Roduner Cattia, Farhat Yamshid, Thöni David, Patel Martin Kumar, Parra David. Spatial analysis of distribution grid capacity and costs to enable massive deployment of PV, electric mobility and electric heating. Appl Energy 2021;287:116504.

[7] Rinaldi Arthur, Yilmaz Selin, Patel Martin K, Parra David. What adds more flexibility? An energy system analysis of storage, demand-side response, heating electrification, and distribution reinforcement. Renew Sustain Energy Rev 2022;167:112696.

[8] Mancarella Pierluigi. MES (multi-energy systems): An overview of concepts and evaluation models. Energy 2014;65:1–17.

[9] Heendeniya Charitha Buddhika, Sumper Andreas, Eicker Ursula. The multi-energy system co-planning of nearly zero-energy districts – status-quo and future research potential. Appl Energy 2020;267:114953.

[10] Sayegh Marderos A, Danielewicz Jan, Nannou Theodora, Miniewicz Maciej, Jadwiszczak Piotr, Piekarska Katarzyna, Jouhara Hussam. Trends of European research and development in district heating technologies. Renew Sustain Energy Rev 2017;68:1183–92.

[11] Pfenninger Stefan, Hawkes Adam, Keirstead James. Energy systems modeling for twenty-first century energy challenges. Renew Sustain Energy Rev 2014;33:74–86.

[12] Haydt Gustavo, Leal Vítor, Pina André, Silva Carlos A. The relevance of the energy resource dynamics in the mid/long-term energy planning models. Renew Energy 2011;36(11):3068–74.

[13] Liu Xuezhi, Mancarella Pierluigi. Modelling, assessment and sankey diagrams of integrated electricity-heat-gas networks in multi-vector district energy systems. Appl Energy 2016;167:336–52.

[14] Salpakari Jyri, Mikkola Jani, Lund Peter D. Improved flexibility with large-scale variable renewable power in cities through optimal demand side management and power-to-heat conversion. Energy Convers Manage 2016;126:649–61.

[15] Widl Edmund, Jacobs Tobias, Schwabeneder Daniel, Nicolas Sebastien, Basciotti Daniele, Henein Sawsan, Noh Tae-Gil, Terreros Olatz, Schuelke Anett, Auer Hans. Studying the potential of multi-carrier energy distribution grids: A holistic approach. Energy 2018;153:519–29.

[16] Schweiger Gerald, Rantzer Jonatan, Ericsson Karin, Laue Patrick. The potential of power-to-heat in Swedish district heating systems. Energy 2017;137:661–9.

[17] Böttger Diana, Götz Mario, Lehr Nelly, Kondziella Hendrik, Bruckner Thomas. Potential of the power-to-heat technology in district heating grids in Germany. Energy Procedia 2014;46:246–53, 8th International Renewable Energy Storage Conference and Exhibition (IRES 2013).

[18] Kontu Kaisa, Rinne Samuli, Junnila Seppo. Introducing modern heat pumps to existing district heating systems – Global lessons from viable decarbonizing of district heating in Finland. Energy 2019;166:862–70.

[19] Capone Martina, Guelpa Elisa, Mancò Giulia, Verda Vittorio. Integration of storage and thermal demand response to unlock flexibility in district multi-energy systems. Energy 2021;237:121601.

[20] Fambri Gabriele, Mazza Andrea, Guelpa Elisa, Verda Vittorio, Badami Marco. Power-to-heat plants in district heating and electricity distribution systems: A techno-economic analysis. Energy Convers Manage 2023;276:116543.

[21] Bordignon Sara, Quaggiotto Davide, Vivian Jacopo, Emmi Giuseppe, De Carli Michele, Zarrella Angelo. A solar-assisted low-temperature district heating and cooling network coupled with a ground-source heat pump. Energy Convers Manage 2022;267:115838.

[22] Lund Henrik, Werner Sven, Wiltshire Robin, Svendsen Svend, Thorsen Jan Eric, Hvelplund Frede, Mathiesen Brian Vad. 4th Generation District Heating (4GDH): Integrating smart thermal grids into future sustainable energy systems. Energy 2014;68:1–11.

[23] Schweiger Gerald, Heimrath Richard, Falay Basak, O'Donovan Keith, Nageler Peter, Pertschy Reinhard, Engel Georg, Streicher Wolfgang, Leusbrock Ingo. District energy systems: Modelling paradigms and general-purpose tools. Energy 2018;164:1326–40.

[24] Saelens Dirk, De Jaeger Ina, Bünning Felix, Mans Michael, Vandermeulen Annelies, van der Heijde Bram, Garreau Enora, Maccarini Alessandro, Rønneseth Øystein, Sartori Igor, Helsen Lieve. Towards a DESTEST : a district energy simulation test developed in IBPSA project 1. In: 16th international conference of the international building performance simulation association (Building Simulation 2019). Building simulation conference proceedings, Vol. 16, Rome: International Building Performance Simulation Association; 2020, p. 3569–76.

[25] Blochwitz Torsten, Otter Martin, Akesson J, Arnold Martin, Clauß C, Elmqvist Hilding, Friedrich M, Junghanns A, Mauss J, Neumerkel D, Olsson H, Viel A. Functional mockup interface 2.0: The standard for tool independent exchange of simulation models. In: Proceedings of the 9th international Modelica conference, Munich, Germany, September 3-5, 2012. 2012.

[26] Erdmann Anselm, Marcellan Anna, Hering Dominik, Suriyah Michael, Ulbrich Carolin, Henke Martin, Xhonneux André, Müller Dirk, Schlatmann Rutger, Hagenmeyer Veit. On verification of designed energy systems using distributed co-simulations. In: 2020 IEEE/ACM 24th international symposium on distributed simulation and real time applications (DS-RT). 2020, p. 235–42.

[27] Chang Miguel, Thellufsen Jakob Zink, Zakeri Behnam, Pickering Bryn, Pfenninger Stefan, Lund Henrik, Østergaard Poul Alberg. Trends in tools and approaches for modelling the energy transition. Appl Energy 2021;290:116731.

[28] Bucher Christof, Betcke Jethro, Andersson Göran. Effects of variation of temporal resolution on domestic power and solar irradiance measurements. In: 2013 IEEE grenoble conference. 2013.

[29] Klemm Christian, Vennemann Peter. Modeling and optimization of multi-energy systems in mixed-use districts: A review of existing methods and approaches. Renew Sustain Energy Rev 2021;135:110206.

[30] Hassan Muhammed A, Khalil Adel, Abubakr Mohamed. Selection methodology of representative meteorological days for assessment of renewable energy systems. Renew Energy 2021;177:34–51.

[31] Müller Dirk, Lauster Moritz, Constantin Ana, Fuchs Marcus, Remmen Peter. AixLib – An open-source Modelica library within the IEA-EBC Annex 60 framework. In: Proceedings of the CESBP Central European Symposium on Building Physics and BauSIM 2016. 2016, p. 3–9.

[32] Thurner Leon, Scheidler Alexander, Schäfer Florian, Menke Jan-Hendrik, Dollichon Julian, Meier Friederike, Meinecke Steffen, Braun Martin. Pandapower—An open-source python tool for convenient modeling, analysis, and optimization of electric power systems. IEEE Trans Power Syst 2018;33(6):6510–21.

[33] Zimmerman Ray Daniel, Murillo-Sánchez Carlos Edmundo, Thomas Robert John. MATPOWER: Steady-state operations, planning, and analysis tools for power systems research and education. IEEE Trans Power Syst 2011;26(1):12–9.

[34] Zornek Timo, Monz Thomas, Aigner Manfred. Performance analysis of the micro gas turbine Turbec T100 with a new FLOX-combustion system for low calorific fuels. Appl Energy 2015;159:276–84.

[35] Bower Hannah E, Schwärzle Andreas, Grimm Felix, Zornek Timo, Kutne Peter. Experimental analysis of a micro gas turbine combustor optimized for flexible operation with various gaseous fuel compositions. J Eng Gas Turbines Power 2020;142(3).

[36] Seliger-Ost Hannah, Kutne Peter, Zanger Jan, Aigner Manfred. Experimental investigation of the impact of biogas on a 3 kW micro gas turbine FLOX®-based combustor. J Eng Gas Turbines Power 2021;143(8).

[37] Krummrein Thomas, Henke Martin, Kutne Peter. A highly flexible approach on the steady-state analysis of innovative micro gas turbine cycles. J Eng Gas Turbines Power 2018;140(12).

[38] Henke Martin, Klempp Nikolai, Hohloch Martina, Monz Thomas, Aigner Manfred. Validation of a T100 micro gas turbine steady-state simulation tool. In: Proceedings of the ASME Turbo Expo, Vol. 3. 2015.

[39] DWD Climate Data Center (CDC). Historical 10-minute station observations of pressure, air temperature (at 5 cm and 2 m height), humidity, dew point, solar incoming radiation, longwave downward radiation, sunshine duration, mean wind speed and wind direction for Germany, version V1. last accessed: Nov 10th, 2021.

[40] Hersbach H, Bell B, Berrisford P, Biavati G, Horányi A, Muñoz Sabater J, Nicolas J, Peubey C, Radu R, Rozum I, Schepers D, Simmons A, Soci C, Dee D, Thépaut J-N. ERA5 hourly data on single levels from 1959 to present. Copernicus climate change service (C3S) climate data store (CDS). 2018, http://dx.doi.org/10.24381/cds.adbb2d47.

[41] Holmgren William F, Hansen Clifford W, Mikofski Mark A. Pvlib python: A python package for modeling solar energy systems. J Open Source Softw 2018;3(29):884–6.

[42] Verband der Elektrotechnik, Elektronik und Informationstechnik (VDE). VDE-AR-N 4105—Technische Mindestanforderungen für Anschluss und Parallelbetrieb von Erzeugungsanlagen am Niederspannungsnetz. VDE-Anwendungsregel, 2018.

[43] Pflugradt Noah, Stenzel Peter, Kotzur Leander, Stolten Detlef. LoadProfileGenerator: An agent-based behavior simulation for generating residential load profiles. J Open Source Softw 2022;7(71):3574–7.

[44] Pflugradt Noah, Muntwyler Urs. Synthesizing residential load profiles using behavior simulation. Energy Procedia 2017;122:655–60, CISBAT 2017 International Conference – Future Buildings & Districts – Energy Efficiency from Nano to Urban Scale.

[45] Statistisches Bundesamt. Wirtschaftsrechnungen – Einkommens- und Verbrauchsstichprobe Wohnverhältnisse privater Haushalte. 2018, Available online [2022-07-11]: https://www.statistischebibliothek.de/mir/receive/DEHeft_mods_00112054.

[46] Loga Tobias, Stein Britta, Diefenbach Nikolaus, Born Rolf. Deutsche Wohngebäudetypologie – Beispielhafte Maßnahmen zur Verbesserung der Energieeffizienz von typischen Wohngebäuden. 2015.

[47] Remmen Peter, Lauster Moritz, Mans Michael, Fuchs Marcus, Osterhage Tanja, Müller Dirk. TEASER: an open tool for urban energy modelling of building stocks. J Build Perform Simul 2018;11(1):84–98.

[48] Kates Robert W, Clark William C, Corell Robert, Hall J Michael, Jaeger Carlo C, Lowe Ian, McCarthy James J, Schellnhuber Hans Joachim, Bolin Bert, Dickson Nancy M, Faucheux Sylvie, Gallopin Gilberto C, Grübler Arnulf, Huntley Brian, Jäger Jill, Jodha Narpat S, Kasperson Roger E, Mabogunje Akin, Matson Pamela, Mooney Harold, Moore III Berrien, O'Riordan Timothy, Svedin Uno. Environment and development: Sustainability science. Science 2001;292(5517):641–2.

[49] Jerneck Anne, Olsson Lennart, Ness Barry, Anderberg Stefan, Baier Matthias, Clark Eric, Hickler Thomas, Hornborg Alf, Kronsell Annica, Lövbrand Eva, Persson Johannes. Structuring sustainability science. Sustain Sci 2011;6(1):69–82.

[50] Bebbington Jan, Larrinaga Carlos. Accounting and sustainable development: An exploration. Account Organ Soc 2014;39(6):395–413.

[51] Evans Annette, Vladimir Strezov V, Evans Tim J. Assessment of sustainability indicators for renewable energy technologies. Renew Sustain Energy Rev 2009;13(5):1082–8.

[52] The European Commission. Comission delegated regulation (EU) No 626/2011. 2011, Available online [2023-03-06] https://data.europa.eu/eli/reg_del/2011/626/oj.

[53] prEN 50160:2021. Voltage characteristics of electricity supplied by public distribution networks. Norm, 2021.

[54] Agora Verkehrswende, Agora Energiewende, Frontier Economics. The future cost of electricity-based synthetic fuels. 2018.

[55] Müller Amelie, Friedrich Lorenz, Reichel Christian, Herceg Sina, Mittag Max, Neuhaus Dirk Holger. A comparative life cycle assessment of silicon PV modules: Impact of module design, manufacturing location and inventory. Sol Energy Mater Sol Cells 2021;230:111277.

[56] Kost Christoph, Shammugam Shivenes, Fluri Verena, Peper Dominik, Memar Aschkan Davoodi, Schlegl Thomas. Fraunhofer ISE, Studie: Stromgestehungskosten erneuerbare Energien. 2021.

[57] Kougias Ioannis, Taylor Nigel, Kakoulaki Georgia, Jäger-Waldau Arnulf. The role of photovoltaics for the European Green Deal and the recovery plan. Renew Sustain Energy Rev 2021;144:111017.

[58] Mengis Nadine, Kalhori Aram, Simon Sonja, Harpprecht Carina, Baetcke Lars, Prats-Salvado Enric, Schmidt-Hattenberger Cornelia, Stevenson Angela, Dold Christian, El Zohbi Juliane, Borchers Malgorzata, Thrän Daniela, Korte Klaas, Gawel Erik, Dolch Tobias, Heß Dominik, Yeates Christopher, Thoni Terese, Markus Till, Schill Eva, Xiao Mengzhu, Köhnke Fiona, Oschlies Andreas, Förster Johannes, Görl Knut, Dornheim Martin, Brinkmann Torsten, Beck Silke, Bruhn David, Li Zhan, Steuri Bettina, Herbst Michael, Sachs Torsten, Monnerie Nathalie, Pregger Thomas, Jacob Daniela, Dittmeyer Roland. Net-zero CO_2 Germany—A retrospect from the year 2050. Earth's Future 2022;10(2).

[59] European Technology & Innovation Platform PhotoVoltaics. Strategic research and innovation agenda on photovoltaics. 2022, www.etip-pv.eu.

[60] Cao Sunliang, Sirén Kai. Impact of simulation time-resolution on the matching of PV production and household electric demand. Appl Energy 2014;128:192–208.

[61] Bögel Paula Maria, Upham Paul, Shahrokni Hossein, Kordas Olga. What is needed for citizen-centered urban energy transitions: Insights on attitudes towards decentralized energy storage. Energy Policy 2021;149:112032.

[62] Tan Kang Miao, Ramachandaramurthy Vigna K, Yong Jia Ying. Integration of electric vehicles in smart grid: A review on vehicle to grid technologies and optimization techniques. Renew Sustain Energy Rev 2016;53:720–32.

[63] Su Chang, Dalgren Johan, Palm Björn. High-resolution mapping of the clean heat sources for district heating in Stockholm City. Energy Convers Manage 2021;235:113983.

[64] Jodeiri Amir M, Goldsworthy Mark J, Buffa Simone, Cozzini Marco. Role of sustainable heat sources in transition towards fourth generation district heating – A review. Renew Sustain Energy Rev 2022;158:112156.